Motion-compensated estimation of delivered dose during external beam radiation therapy: Implementation in Philips' Pinnacle^3 treatment planning system

Shyam Bharat
Philips Medical Systems, Fitchburg, Wisconsin 53711

Parag Parikh[a)] and Camille Noel
Department of Radiation Oncology, Washington University in St. Louis School of Medicine, St. Louis, Missouri 63110

Michael Meltsner, Karl Bzdusek, and Michael Kaus
Philips Medical Systems, Fitchburg, Wisconsin 53711

(Received 27 July 2011; revised 25 October 2011; accepted for publication 23 November 2011; published 28 December 2011)

Purpose: Recent research efforts investigating dose escalation techniques for three-dimensional conformal radiation therapy (3D CRT) and intensity modulated radiation therapy (IMRT) have demonstrated great benefit when high-dose hypofractionated treatment schemes are implemented. The use of these paradigms emphasizes the importance of smaller treatment margins to avoid high dose to surrounding normal tissue or organs at risk (OARs). However, tighter margins may lead to underdosage of the target due to the presence of organ motion. It is important to characterize organ motion and possibly account for it during treatment delivery. The need for real-time localization of dynamic targets has encouraged the use and development of more continuous motion monitoring systems such as kilo-voltage/fluoroscopic imaging, electromagnetic tracking, and optical monitoring systems.
Methods: This paper presents the implementation of an algorithm to quantify translational and rotational interfractional and intrafractional prostate motion and compute the dosimetric effects of these motion patterns. The estimated delivered dose is compared with the static plan dose to evaluate the success of delivering the plan in the presence of prostate motion. The method is implemented on a commercial treatment planning system (Pinnacle^3, Philips Radiation Oncology Systems, Philips Healthcare) and is termed delivered dose investigational tool (DiDIT). The DiDIT implementation in Pinnacle^3 is validated by comparisons with previously published results. Finally, different workflows are discussed with respect to the potential use of this tool in clinical treatment planning.
Results: The DiDIT dose estimation process took approximately 5–20 min (depending on the number of fractions analyzed) on a Pinnacle^3 9.100 research version running on a Dell M90 system (Dell, Inc., Round Rock, TX, USA) equipped with an Intel Core 2 Duo processor (Intel Corporation, Santa Clara, CA, USA). The DiDIT implementation in Pinnacle^3 was found to be in agreement with previously published results, on the basis of the percent dose difference (PDD). This metric was also utilized to compare plan dose versus delivered dose, for prostate targets in three clinically acceptable treatment plans.
Conclusions: This paper presents results from the implementation of an algorithm on a commercially available treatment planning system that quantifies the dosimetric effects of interfractional and intrafractional motion in external beam radiation therapy (EBRT) of prostate cancer. The implementation of this algorithm within a commercial treatment planning system such as Pinnacle^3 enables easy deployment in the existing clinical workflow. The results of the PDD tests validate the implementation of the DiDIT algorithm in Pinnacle^3, in comparison with previously published results. [DOI: 10.1118/1.3670374]

Key words: external beam radiation therapy, adaptive treatment planning and delivery, intrafraction organ motion, Pinnacle, electromagnetic tracking, delivered dose estimation

I. INTRODUCTION

External beam radiation therapy (EBRT) is one of the primary methods of treatment for many patients afflicted with cancer. The process of EBRT generally involves a multifaceted workflow, including pretreatment imaging (usually computed tomography (CT) simulation), image-based treatment planning, and fractionated treatments spread over multiple days. Since simulation and treatment are separated by days or weeks, geometric uncertainties due to gradual anatomical variations, organ motion, and set-up errors can present significant obstacles in the successful delivery of the plan. The traditional way to account for these uncertainties is to include additional treatment margins—the planning

target volume (PTV)—around the clinical target volume (CTV) to allow for patient set-up errors, organ motion, and other geometric uncertainties. Thus, the actual treated region usually includes not just the originally defined tumor but a larger surrounding region of tissue. It is also important to note that margins are typically defined according to population-based studies or historical literature, and are not patient-specific.

The main trade-off encountered in EBRT is the need for complete tumor destruction while simultaneously sparing surrounding normal tissue and/or organs at risk (OARs) from radiation. Treating with smaller margins will consequently allow dose escalation in the target. Dose escalation has been shown to result in improved clinical outcomes for prostate cancer patients.[1,2] In recent years, many research efforts have focused on tightening treatment margins to spare surrounding normal tissue and/or OARs, while at the same time ensuring complete target coverage.[3–5] Refined models of interfractional and intrafractional target motion relative to surrounding anatomy are required for this. However, methods of estimating and compensating for these more detailed motion models are not yet standard practice in many clinical institutions. Hence, the need to estimate target motion before and during treatment and utilize this information to optimize treatment plans is becoming of paramount importance.

Various image-based techniques have been used to quantify interfractional prostate motion at various stages of radiation treatment delivery, e.g., weekly CT imaging,[6] daily cone beam CT (Ref. 7), etc. Fiducial markers implanted in the prostate, in conjunction with fluoroscopic imaging, are being increasingly used to obtain motion information.[8–10] The key assumption when relying on fiducial marker-based positional information is that the prostate can be considered to be a rigid body.[11] Deformation, though present in the prostate, has been shown to be rather small in magnitude (<0.5 mm).[12–14] Rigid motion consists of two components: translation and rotation. There exist methods to quantify the translational components of prostate motion and estimate the resulting dosimetric effects.[15,16] The rotational components of intrafractional motion have been quantified previously,[17,18] but their dosimetric implications have not been studied widely. A recent publication has shown that conclusions about the success (or otherwise) of dose delivery may not be accurate if rotations are not accounted for Ref. 19.

A recent publication presented a method to estimate the dosimetric effect of translational and rotational components of intrafractional prostate motion using positional information obtained with electromagnetic (EM) fiducials in the prostate.[20] Positional information of the fiducials, used as a surrogate for the prostate, was obtained at a high temporal frequency during delivery of all treatment fractions, thus, affording the ability to quantify both interfractional and intrafractional rigid motion. A MATLAB-based (The Mathworks, Natick, MA, USA) application called Semi-Automatic Workflow using Intrafraction Fiducial-based Tracking for Evaluation of Radiotherapy (SWIFTER) was used to accumulate the dose delivered to the prostate, which was retrospectively compared with the static plan dose.

In this paper, the implementation of this method of dose estimation in Pinnacle[3], a commercially available treatment planning system (Philips Medical Systems, Fitchburg, WI, USA), is described and is termed delivered dose investigational tool (DiDIT). While any point-based motion acquisition method can be integrated into DiDIT, electromagnetic fiducial motion data were used here to correspond with methodology used in Noel *et al.*[20] The implementation was tested on treatment plans with different PTV margins (5, 3, and 0 mm) and compared with results from SWIFTER.[20] Methods of clinical implementation of this tool are also discussed.

II. METHODS AND MATERIALS

II.A. Workflow

The motion estimation method employed here utilizes positional information from electromagnetic transponders (Calypso 4D Localization System—Calypso Medical Systems®, Seattle, WA) implanted in the prostate, as a surrogate for the target. The Calypso® system tracks the spatial coordinates of each of the three transponders in succession at 10 Hz. The algorithm calculates the rigid motion (translation + rotation) between the transponder positions at any given instant and the transponder positions in the planning CT scan. Translation is calculated as the distance between the centroids of the two orientations of the transponders. After accounting for the translation, the transponders are assumed to only differ by a rotation. This rotation is divided into three rotational components: the pitch, yaw and roll, i.e., rotations about the L-R (X) axis, A-P (Y) axis and S-I (Z) axis, respectively. The estimated translations and rotations are inserted into bins (1 mm bins for the translations and 1° bins for the rotations). This information is used to generate a probability density function (PDF) of spatial existence for each voxel, over the entire period of radiation delivery. This PDF represents the percentage of time spent by that voxel at any given spatial location. Finally, the PDFs thus constructed are convolved with the static plan dose grid to derive the estimated delivered dose grid. Figure 1 illustrates the above workflow.

II.B. Motion estimation algorithm

The estimation algorithm employed here is an iterative method that utilizes the traditional least squares formalism to estimate three successive rotations about the Cartesian coordinate axes, in addition to a single translation.[20] The least squares minimization routine is utilized to calculate the "best fit" between the observed data (current transponder coordinates, i.e., CTCs) and the least squares model which is known *apriori*.

Consider the following observation model:

$$y = H\theta + n,$$

where $y = (y_1, y_2, \ldots, y_N)^T$ is the observation vector, $\theta = (\theta_1, \theta_2, \ldots, \theta_P)^T$ is the quantity to be estimated, H is a known $N \times P$ real matrix of regressors, and n is the noise vector $(N \times 1)$.

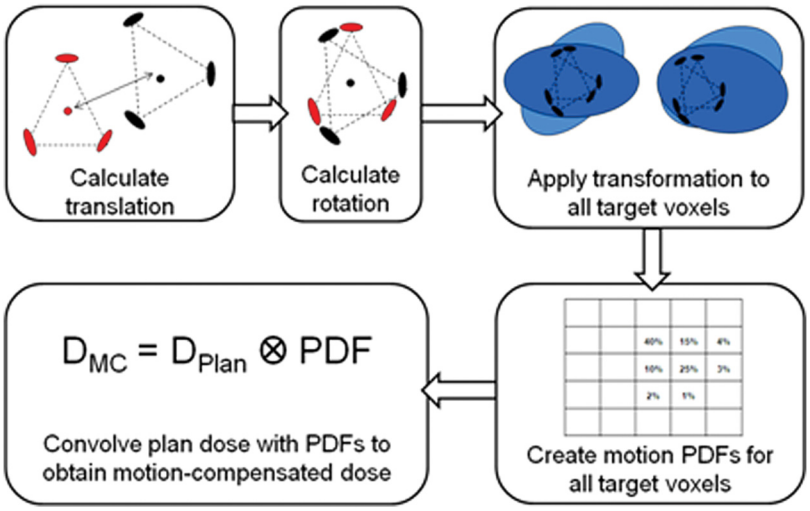

FIG. 1. The workflow of the DiDIT algorithm.

The squared error between y and the model Hθ' is minimized

$$\varepsilon^2 = (\mathrm{y} - \mathrm{H}\theta')^{\mathrm{T}}(\mathrm{y} - \mathrm{H}\theta').$$

Therefore, $-2\mathrm{H}^{\mathrm{T}}(\mathrm{y} - \mathrm{H}\theta') = 0$

$$\theta' = (\mathrm{H}^{\mathrm{T}}\mathrm{H})^{-1}\mathrm{H}^{\mathrm{T}}\mathrm{y},$$

where $\theta = [\theta_{\mathrm{x}}\ \theta_{\mathrm{y}}\ \theta_{\mathrm{z}}]$ refers to the rigid motion parameters (the rotation angles, i.e., pitch, yaw and roll) that need to be estimated.

There are three rotation matrices, corresponding to the pitch (θ_{x}), yaw (θ_{y}), and roll (θ_{z}), respectively.

$$R(\theta_x) = \begin{bmatrix} 1 & 0 & 0 \\ 0 & \cos\theta_x & -\sin\theta_x \\ 0 & \sin\theta_x & \cos\theta_x \end{bmatrix},$$

$$R(\theta_y) = \begin{bmatrix} \cos\theta_y & 0 & \sin\theta_y \\ 0 & 1 & 0 \\ -\sin\theta_y & 0 & \cos\theta_y \end{bmatrix},$$

$$R(\theta_z) = \begin{bmatrix} \cos\theta_z & -\sin\theta_z & 0 \\ \sin\theta_z & \cos\theta_z & 0 \\ 0 & 0 & 1 \end{bmatrix}.$$

The effective rotation matrix can be calculated from the individual rotation matrices as:

$$\mathrm{R}(\theta_{\mathrm{x}}, \theta_{\mathrm{y}}, \theta_{\mathrm{z}}) = \mathrm{R}(\theta_{\mathrm{x}})^{*}\ \mathrm{R}(\theta_{\mathrm{y}})^{*}\ \mathrm{R}(\theta_{\mathrm{z}})$$

The transformation matrix is constructed from the rotation matrix $\mathrm{R}(\theta_{\mathrm{x}},\theta_{\mathrm{y}},\theta_{\mathrm{z}})$ as

$$A(\theta_x, \theta_y, \theta_z) = \begin{bmatrix} & & & trans.\ x \\ R(\theta_x, \theta_y, \theta_z) & & & trans.\ y \\ & & & trans.\ z \\ 0 & 0 & 0 & 1 \end{bmatrix}.$$

Each voxel of the target is then transformed as follows:

$$\mathrm{V}_{\mathrm{post}} = \mathrm{V}_{\mathrm{pre}} * \mathrm{A}(\theta_{\mathrm{x}}, \theta_{\mathrm{y}}, \theta_{\mathrm{z}}).$$

Note that only voxels belonging to the target can be transformed because the transformations calculated are from the motion of the transponders, which are a surrogate for only the target or organ in which they are implanted. The motion parameters calculated from the transponders should not be applied to voxels belonging to surrounding organs.

II.C. Dose convolution

The motion estimation procedure is performed on the entire data set (containing tracking data from all treatment fractions) to generate spatial PDFs for each voxel belonging to the target. These spatial PDFs represent the percentage of time spent by that voxel in a given region of space, in the Pinnacle[3] frame of reference. The static plan dose distribution is then convolved with these PDFs to generate the dose distribution actually delivered to the patient.

II.D. Performance validation

A recent paper by Noel *et al*. detailed the use of a software application, SWIFTER, to retrospectively analyze dosimetric target coverage by quantifying rigid motion of the target from all treatment fractions.[20] The results obtained from DiDIT compared favorably with the results from SWIFTER. Three treatment plans with different PTV margins (5, 3, and 0 mm) were utilized for this comparison study. Comparisons were drawn on the basis of the following criteria:

Dose values: The minimum dose, average dose, and maximum dose within the prostate were compared for the delivered dose grids resulting from DiDIT and SWIFTER.

Voxel differences: The percent dose difference (PDD) is an important quantity that is routinely analyzed to determine dosimetric equivalence.[21] The difference dose between the two dose grids were analyzed for the average difference. Histograms of the absolute values of the differences are presented.

II.E. Delivered dose versus planned dose

The estimated delivered dose is compared with the planned dose distribution, to test for successful delivery of the treatment plan. A prostate cancer patient's treatment plan

TABLE I. Minimum, average, and maximum dose voxel values in the prostate, for estimated delivered dose grids resulting from DiDIT and SWIFTER.

	5 mm margin			3 mm margin			0 mm margin		
Delivered dose parameters	Plan	DiDIT	SWIFTER	Plan	DiDIT	SWIFTER	Plan	DiDIT	SWIFTER
Minimum dose (Gy)	74.9	75.2	75	74.3	74.6	73.6	71.4	67.8	67.1
Average dose (Gy)	77.2	77.2	77.2	77.5	77.4	77.5	76.3	76.4	75.9
Maximum dose (Gy)	79.7	79.1	79.5	79.9	79.4	79.7	79.2	79	79.1

generated using a standard seven-field intensity modulated radiation therapy (IMRT) paradigm with 5 mm PTV margins is utilized. The prescription dose was 76 Gy delivered over 41 fractions at an energy of 18 MV. Two additional treatment plans are tested, each with differently-sized PTV margins (3 and 0 mm margins). Comparisons are drawn on the basis of the PDD and dose volume histograms (DVH). The PDD curve is two-sided, so that information can be garnered about the magnitude of both cold spots and hot spots, if any.

The three treatment plans evaluated consisted of different PTV margins on which the dose optimization was performed. The 5 mm PTV margin is the traditionally used margin in the clinic to account for patient set-up errors, geometric uncertainties, and organ motion before and during radiation treatment delivery. The 3 and 0 mm PTV margins were used to evaluate the effect of organ motion and other geometric uncertainties on the dose delivered to the patient, for treatment margins smaller than the conventional 5 mm margin.

III. RESULTS

The DiDIT dose estimation process took approximately 5–20 min (depending on number of fractions analyzed) on a Pinnacle^3 9.100 research version running on a Dell M90 system (Dell, Inc., Round Rock, TX, USA) equipped with an Intel Core 2 Duo processor (Intel Corporation, Santa Clara, CA, USA). Table I displays comparisons between the minimum, average, and maximum dose voxel values in the prostate, for estimated delivered dose grids resulting from DiDIT and SWIFTER. Table II displays comparisons between the results of the DiDIT implementation and those of the SWIFTER application, in terms of the PDD for the 5, 3, and 0 mm margin treatment plans. Previous studies have determined that a PDD in the range of 2%–4% indicates dosimetric equivalence between the quantities being compared.[21] The average PDD values for the 5, 3, and 0 mm margin plans were 0.23%, 0.39%, and 0.43%, respectively, all of which are less than the lower end of the stated 2%–4% range. All the target voxels in the 5 and 3 mm margin plans differed by less than 4%, while 99.95% of the target voxels in the 0 mm margin plan differed by less than 4%. When the threshold was dropped to 2%, this criterion was still satisfied by all

TABLE II. Comparison using PDD values between the results of DiDIT and SWIFTER, for the 5 mm, 3 mm, and 0 mm margin plans, respectively.

Percent dose difference (PDD)	5 mm margin	3 mm margin	0 mm margin
Average PDD (%)	0.2	0.4	0.4
Maximum PDD (%)	1.1	2.2	5.2
Standard deviation (%)	0.2	0.3	0.5
% of voxels with PDD < 4%	100	100	99.9
% of voxels with PDD < 3%	100	100	99.7
% of voxels with PDD < 2%	100	999	98.5

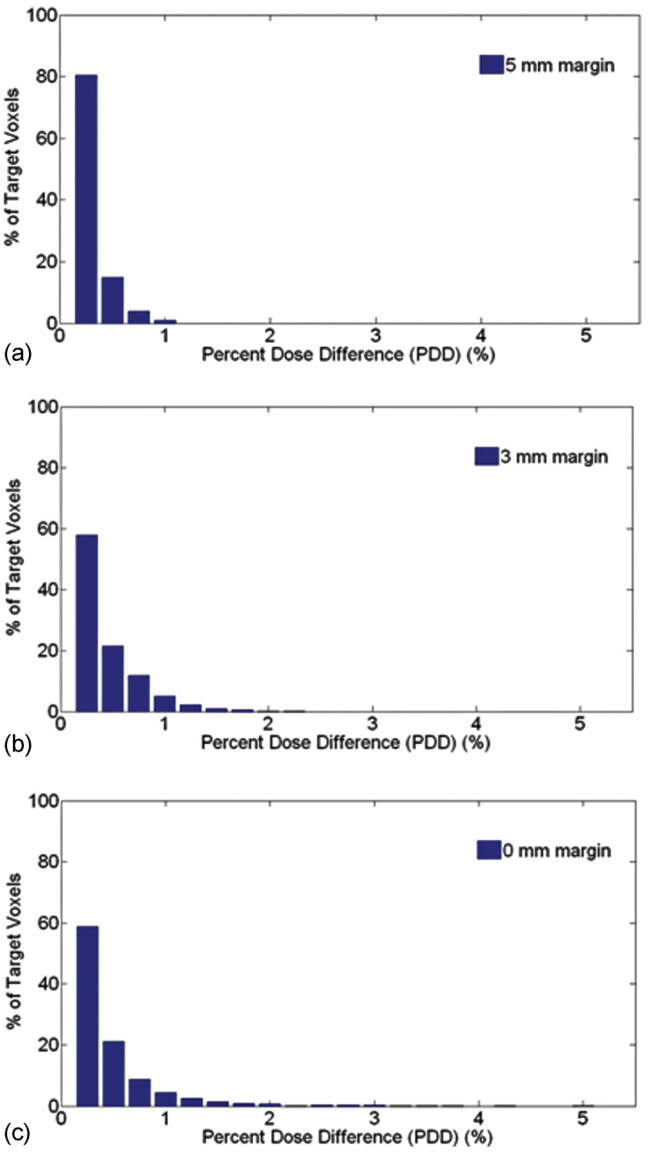

FIG. 2. (a) Histograms of PDD values between the results of DiDIT and SWIFTER, for the 5 mm margin plans (b) histograms of PDD values between the results of DiDIT and SWIFTER, for the 3 mm margin plans and (c) histograms of PDD values between the results of DiDIT and SWIFTER, for the 0 mm margin plans.

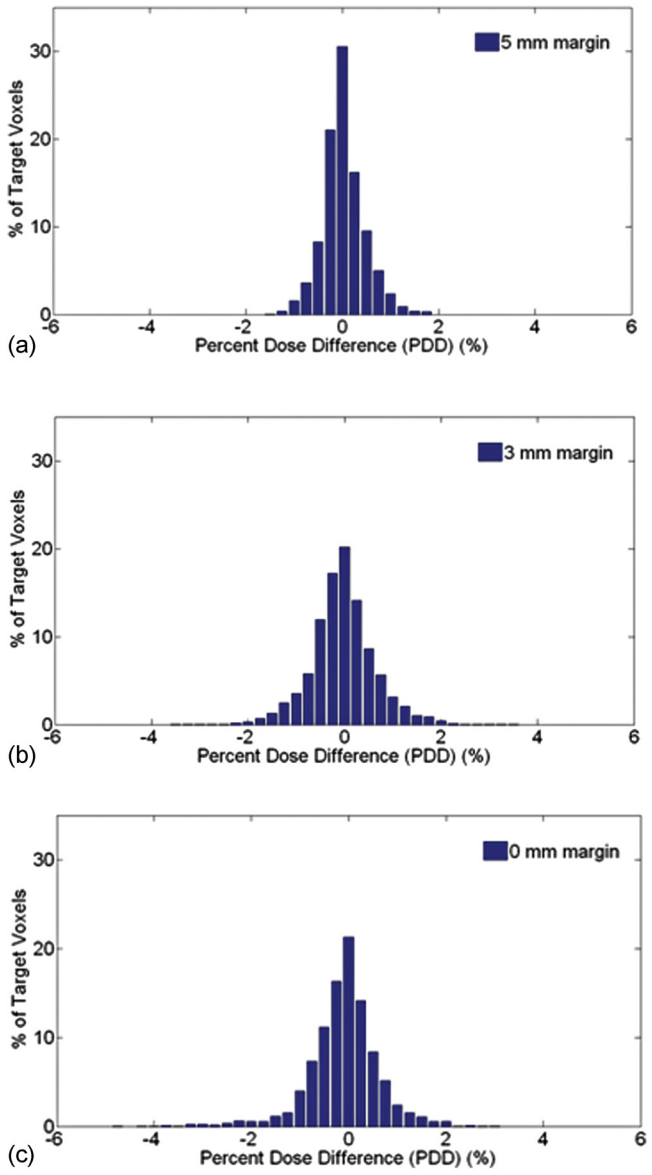

FIG. 3. (a) Histograms of PDD values between the original plan dose distribution and the results of DiDIT, for the 5 mm margin plans (b) Histograms of PDD values between the original plan dose distribution and the results of DiDIT, for the 3 mm margin plans and (c) histograms of PDD values between the original plan dose distribution and the results of DiDIT, for the 0 mm margin plans.

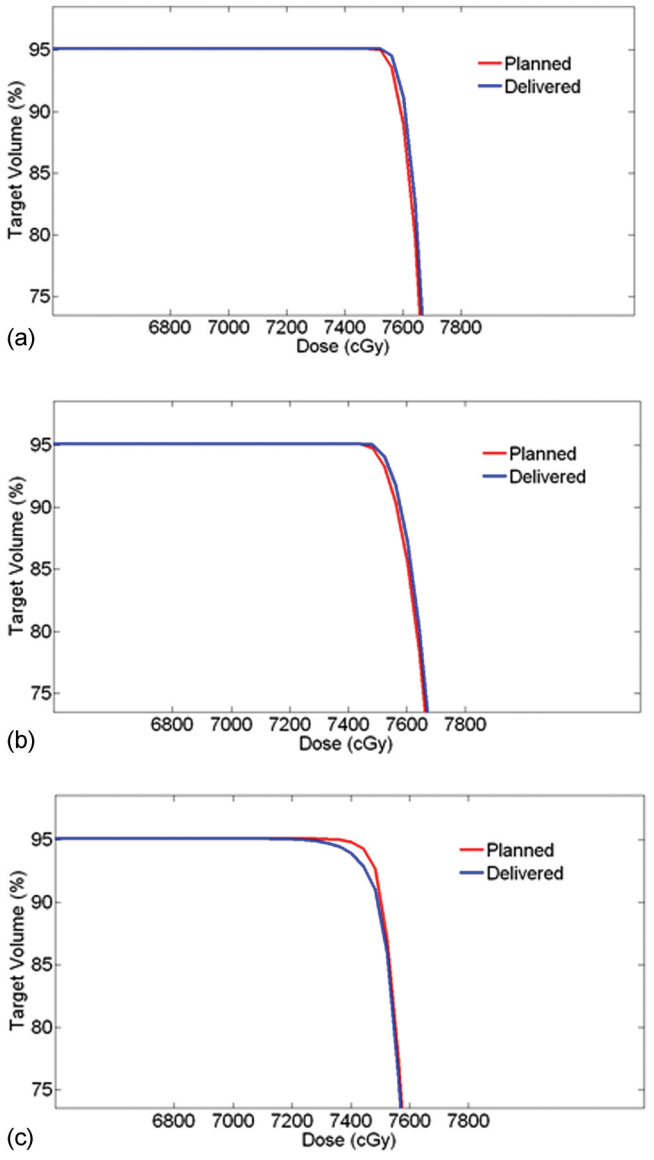

FIG. 4. (a) DVHs for the 5 mm margin plans (b) DVHs for the 3 mm margin plans and (c) DVHs for the 0 mm margin plans.

target voxels in the 5 mm margin plan. For the 3 and 0 mm margin plans, 99.87% and 98.52% of the target voxels were within 2% agreement, respectively. Figures 2(a)–2(c) plot the percentage of target voxels against the PDD for the 5, 3, and 0 mm margin treatment plans, respectively.

Figures 3(a)–3(c) display PDD histograms for comparison between the original planned dose distribution and the result of DiDIT (i.e., estimated delivered dose distribution). Negative PDD values represent voxels in the delivered dose distribution that are "colder" than the corresponding voxels in the planned dose distribution, while positive PDD values represent voxels in the delivered dose distribution that are "hotter" than the corresponding voxels in the planned distribution. The PDD histograms indicate that dosimetric differences between the planned and delivered dose distributions were the lowest for the 5 mm margin treatment plan, while they were comparatively higher for the 0 mm margin plan. However, even for the 0 mm margin plan, almost all the PDD values lay in the 0%–4% range (in an absolute sense). Based on prior published conclusions, this might be construed as dosimetric equivalence between the planned and delivered dose distributions.[20]

Figures 4(a)–4(c) plot the DVHs for the 5, 3, and 0 mm margin treatment plans, respectively. Figures 4(a) and 4(b) for the 5 and 3 mm margin plans indicate almost overlapping DVH characteristics between the planned and delivered dose distributions. Figure 4(c) shows that, for the 0 mm margin plan, there was a slight dosimetric mismatch near the lower dose regions in the target between the planned and delivered dose distributions. Both the PDD and DVH characteristics might be important tools in the evaluation and analysis of the delivered dose distribution.

IV. DISCUSSION

This paper presents results from the implementation of an algorithm on a commercially available treatment planning system that quantifies the dosimetric effects of interfractional and intrafractional motion in EBRT of prostate cancer. The results of the PDD tests validate implementation of the DiDIT algorithm in Pinnacle^3, in comparison with previously published results by Noel *et al.*[20] The implementation of this algorithm within a commercial treatment planning system such as Pinnacle^3 enables easy deployment in the existing clinical workflow.

Here, we demonstrate its usage for prostate cancer patients using electromagnetic fiducial-based tracking; however, DiDIT is designed to utilize any form of point-based localization information in one to three spatial dimensions. This includes positional data acquired from implanted fiducials or anatomical landmarks visualized during image-guided RT on kV and MV imaging, fluoroscopy, cone beam CT, megavoltage CT, ultrasound, and magnetic resonance imaging. Point-based surface tracking systems such as VisionRT® (London, UK) can provide interfractional and intrafractional positional information that would be ideal for utilizing DiDIT for evaluation of breast cancer treatment. It must be noted that the DiDIT algorithm in the present version does not correlate the time stamps of motion with the dose delivery, an aspect that represents the future extension of this work.

DiDIT's integration within a commercial treatment planning system allows easy clinical accessibility. The point-based analysis that DiDIT employs translates to faster processing speeds than volumetric analysis. Estimates of the delivered dose can be available in as little as 5 min, depending on the number of fractions being processed. This allows for quick motion-compensated dosimetry pretreatment (for set-up error analysis) and/or post-treatment (for intrafractional analysis) on a daily basis. Furthermore, DiDIT accounts for target rotations in addition to translations, which is often neglected when reviewing tumor motion.

The tradeoff to the advantage of quick and easy analysis is that point-based tracking provides limited information about target deformation and positions of nearby organs at risk compared to 3D volumetric data. However, this information could be deduced with an adequate number of spatial data points. The number of points considered "adequate" is certainly dependent upon the target site and the amount of information desired. The data used in this study were sourced from a protocol in which three transponders were implanted in the prostate as a surrogate for the tumor. While three is the minimum number of spatial data points required for the motion estimation method presented here, a previous study has shown that the use of four fiducials (the study utilized fiducial markers and not EM transponders) enhances the accuracy of the resulting motion estimates.[22] However, it is unreasonable to assume that fiducial information perfectly reflects volumetric information, which limits what can be concluded about organ deformation. The estimation algorithm described here is based on the assumption that the intertransponder distances remain constant during treatment. Some researchers have shown that the prostate may shrink over time during treatment.[23] Any resulting transponder migration may interfere with the performance of this algorithm.

Our analysis leads us to conclude that motion-compensated dosimetry is not only site-specific, but also patient-specific. Previous work performed by Olsen *et al.* using the SWIFTER application found considerable variation in motion-compensated dosimetry for prostate cancer patients displaying the same general characteristics and treatment schemes.[24] The authors concluded that different margins were appropriate for different patients, and that SWIFTER was important in indentifying individualized margin adequacy. A basic comparison between the plan dose parameters and estimated delivered dose parameters (Table I) indicates that the 0 mm margin treatment plan is more susceptible to motion than the 3 and 5 mm margin treatment plans. This confirms our expectation that the 0 mm margin plan, with its higher dose gradients, would be dosimetrically more intolerant of motion than a corresponding 5 mm margin plan. This tool could potentially be used to build a knowledge database that can help determine which organ geometries, patient characteristics, etc. would be best suited to a 3 mm margin (or even a 0 mm margin), since margin reduction is becoming one of the crucial requirements of hypofractionation schemes to avoid increased dosage to OARs and normal tissue.

We envisage two broad ways in which the motion-compensation algorithm described here can be utilized to improve the existing clinical workflow. The first way is to use the tool retrospectively at the end of the treatment course to analyze the cumulative radiation dose delivered to the patient. The estimated delivered dose can potentially be related to the input parameters of the treatment plan (e.g., contours, treatment margins, beam orientations, beam energies, optimization constraints, etc.) and stored in a database. This database can then be used to prospectively devise optimized treatment plans for future patients. The second approach with respect to the use of this dose estimation tool would be to intervene at one or more stages during the treatment course of a patient. A simple implementation of localization intervention could involve a pretreatment verification via a predetermined range of acceptable patient-specific setup errors (assessed by prospective dosimetric analysis), or a quick DiDIT analysis using actual setup errors at the time of patient localization on the treatment machine. This is most relevant for rotational errors which are often difficult to correct. A more complex implementation of treatment intervention enabled by DiDIT involves the assessment and modification of inadequate treatment plans. The motion information from all previously delivered fractions can be utilized during any point in the treatment course to estimate the cumulative dose delivered. This dose can be compared with the treatment plan that only takes into account those fractions. Because the dose over a subset of the fractions can be summed linearly with minimal radiobiology-based distortions,[25] DiDIT can provide the user with an estimation of the adequacy of the treatment to-date. If the dosimetric differences between the planned and delivered dose are determined to be clinically significant, steps may be taken to re-image and adapt the original treatment plan for the remaining fractions.

The number of radiotherapy systems offering interfractional and intrafractional point-based tumor localization continues to grow, creating a source of valuable data that can be used to offer indications of treatment quality. DiDIT builds upon previous work to enable prospective and retrospective patient-specific dosimetric analysis for dynamic targets influenced by continuous motion, or simple day-to-day positional variations. DiDIT is fast, automated, and offers unique clinical accessibility via integration with a widely-used commercial treatment planning system.

ACKNOWLEDGMENT

Supported by RO1 CA134541-01.

[a]Author to whom correspondence should be addressed. Electronic mail: pparikh@radonc.wustl.edu

[1]A. Pollack *et al.*, "Prostate cancer radiation dose response: Results of the M.D. Anderson phase III randomized trial," Int. J. Radiat. Oncol., Biol., Phys., **53**, 1097–1105 (2002).
[2]A. Zietman *et al.*, "Comparison of conventional-dose vs high-dose conformal radiation therapy in clinically localized adenocarcinoma of the prostate: A randomized controlled trial," JAMA **294**, 1233–1239 (2005).
[3]S. Molinelli *et al.*, "Simultaneous tumour dose escalation and liver sparing in stereotactic body radiation therapy (SBRT) for liver tumours due to CTV-to-PTV margin reduction," Radiother. Oncol. **87**, 432–438 (2008).
[4]H. Sandler *et al.*, "Reduction in patient-reported acute morbidity in prostate cancer patients treated with 81-Gy Intensity-modulated radiotherapy using reduced planning target volume margins and electromagnetic tracking: assessing the impact of margin reduction study," Urology **75**, 1004–1008 (2010).
[5]D. Skarsgard *et al.*, "Planning target volume margins for prostate radiotherapy using daily electronic portal imaging and implanted fiducial markers," Radiat. Oncol. **10**, 52–62 (2010).
[6]K. Deurloo *et al.*, "Quantification of shape variation of prostate and seminal vesicles during external beam radiotherapy," Int. J. Radiat. Oncol., Biol., Phys. **61**, 228–238 (2005).
[7]T. Li *et al.*, "On-line adaptive radiation therapy: feasibility and clinical study," J Oncol. (2010).
[8]C. Beltran *et al.*, "Planning target margin calculations for prostate radiotherapy based on intrafraction and interfraction motion using four localization methods," Int. J. Radiat. Oncol., Biol., Phys. **70**, 289–295 (2008).
[9]H. Dehnad *et al.*, "Clinical feasibility study for the use of implanted gold seeds in the prostate as reliable positioning markers during megavoltage irradiation," Radiother. Oncol. **67**, 295–302 (2003).
[10]D. Litzenberg *et al.*, "Influence of intrafraction motion on margins for prostate radiotherapy," Int. J. Radiat. Oncol., Biol., Phys. **65**, 548–553 (2006).
[11]E. Kerkhof *et al.*, "Variation in target and rectum dose due to prostate deformation: An assessment by repeated MR imaging and treatment planning," Phys. Med. Biol. **53**, 5623–5634 (2008).
[12]P. Kupelian *et al.*, "Intraprostatic fiducials for localization of the prostate gland: Monitoring intermarker distances during radiation therapy to test for marker stability," Int. J. Radiat. Oncol., Biol., Phys. **62**, 1291–1296 (2005).
[13]A. Nichol *et al.*, "A magnetic resonance imaging study of prostate deformation relative to implanted gold fiducial markers," Int. J. Radiat. Oncol., Biol., Phys. **67**, 48–56 (2007).
[14]L. Santanam *et al.*, "Fiducial-based translational localization accuracy of electromagnetic tracking system and on-board kilovoltage imaging system," Int. J. Radiat. Oncol., Biol., Phys. **70**, 892–899 (2008).
[15]H. Li *et al.*, "Dosimetric consequences of intrafraction prostate motion," Int. J. Radiat. Oncol., Biol., Phys. **71**, 801–812 (2008).
[16]P. van Haaren *et al.*, "Influence of daily setup measurements and corrections on the estimated delivered dose during IMRT treatment of prostate cancer patients," Radiother. Oncol. **90**, 291–298 (2009).
[17]M. van Herk *et al.*, "Quantification of organ motion during conformal radiotherapy of the prostate by three dimensional image registration," Int. J. Radiat. Oncol., Biol., Phys. **33**, 1311–1320 (1995).
[18]P. Remeijer *et al.*, "Margins for translational and rotational uncertainties: A probability-based approach," Int. J. Radiat. Oncol., Biol., Phys. **53**, 464–474 (2002).
[19]H. Amro *et al.*, "The dosimetric impact of prostate rotations during electromagnetically guided external beam radiation therapy," Med. Phys. **38**, 3781 (2011).
[20]C. Noel *et al.*, "An automated method for adaptive radiation therapy for prostate cancer patients using continuous fiducial-based tracking," Phys. Med. Biol. **55**, 65–82 (2010).
[21]H. Jin *et al.*, "A generalized a priori dose uncertainty model of IMRT delivery," Med. Phys. **35**, 982–996 (2008).
[22]M. Murphy, "Fiducial-based targeting accuracy for external-beam radiotherapy," Med. Phys. **29**, 334–344 (2002).
[23]T. Budiharto *et al.*, "A semi-automated 2D/3D marker-based registration algorithm modelling prostate shrinkage during radiotherapy for prostate cancer," Radiother. Oncol. **90**, 331–336 (2009).
[24]J. Olsen *et al.*, "Practical method of adaptive radiotherapy for prostate cancer using real-time electromagnetic tracking," Int. J. Radiat. Oncol., Biol., Phys. (in press).
[25]J. Orban de Xivry *et al.*, "Evaluation of the radiobiological impact of anatomic modifications during radiation therapy for head and neck cancer: Can we simply summate the dose?" Radiother. Oncol. **96**, 131–138 (2010).